JOURNAL OF PETROLOGY | VOLUME 45 | NUMBER 11 | PAGES 2287–2302 | 2004 | doi:10.1093/petrology/egh056

# Crustal Growth by Magmatic Accretion Constrained by Metamorphic *P–T* Paths and Thermal Models of the Kohistan Arc, NW Himalayas

**TAKASHI YOSHINO[1]* AND TAKAMOTO OKUDAIRA[2]**

[1]INSTITUTE FOR STUDY OF THE EARTH'S INTERIOR, OKAYAMA UNIVERSITY, YAMADA 827, MISASA, TOTTORI 682-0193, JAPAN

[2]DEPARTMENT OF GEOSCIENCES, GRADUATE SCHOOL OF SCIENCE, OSAKA CITY UNIVERSITY, 3-3-138 SUGIMOTO, OSAKA 558-8585, JAPAN

**RECEIVED APRIL 25, 2003; ACCEPTED JULY 1, 2004**
**ADVANCE ACCESS PUBLICATION AUGUST 27, 2004**

*Magmatic accretion is potentially an important mechanism in the growth of the continental crust and the formation of granulites. In this study, the thermal evolution of a magmatic arc in response to magmatic accretion is modeled using numerical solutions of the one-dimensional heat conduction equation. The initial and boundary conditions used in the model are constrained by geological observations made in the Kohistan area, NW Himalayas. Taking consideration of the preferred intrusion locations for basaltic magmas, we consider two plausible modes of magmatic accretion: the first involves the repeated intrusion of basalt at mid-crustal depths ('intraplate model'), and the second evaluates the simultaneous intrusion of basalt and picrite at mid-crustal depths and the base of the crust respectively ('double-plate model'). The results of the double-plate model account for both the inferred metamorphic* P–T *paths of the Kohistan mafic granulites and the continental geotherm determined from peak* P–T *conditions observed for granulite terranes. The double-plate model may be applicable as a key growth process for the production of thick mafic lower crust in magmatic arcs.*

KEY WORDS: *thermal model; magmatic underplating;* P–T *path; granulite; lower crust*

## INTRODUCTION

Magmatic underplating by basaltic magma derived from the mantle has long been considered an important process in the growth of continental crust and the formation of granulites. The seismic velocity and Poisson's ratio of the lower crust of magmatic arcs and stable Proterozoic cratons indicate a predominantly mafic composition and suggest the existence of a thick (*c.* >10 km) mafic layer (e.g. Nelson, 1991; Holbrook *et al.*, 1992; Rudnick & Fountain, 1995; Zandt & Ammon, 1995). These observations suggest that basaltic underplating is a widespread process. However, most granulite terranes, which are generally regarded as representative of conditions in the lower crust (Fountain & Salisbury, 1981), differ in composition from lower-crustal mafic xenoliths (Rudnick *et al.*, 1986; Rudnick, 1992). This is probably because of the mechanical difficulty in exhuming large volumes of high-density, deep-seated mafic crust. As a general observation, granulite xenoliths, dominated by basaltic compositions, tend to equilibrate at greater depth than regional granulites.

According to previous studies (England & Thompson, 1984; Bohlen & Mezger, 1989; Harley, 1989), there are two important mechanisms for producing granulites: crustal thickening during continental collision and magmatic underplating. Bohlen & Mezger (1989) concluded that crustal thickening by mafic magma crystallization at the crust–mantle boundary might account for both the formation of regional granulite terranes at shallower depths (<30 km) and the formation of the deep-seated mafic crust represented by xenolith suites. The peak

*Corresponding author. Present address: Department of Earth and Environmental Sciences, Rensselaer Polytechnic Institute, Troy, NY 12180, USA. Telephone: +1-518-276-8827. Fax: +1-518-276-2012. E-mail: yoshta@rpi.edu

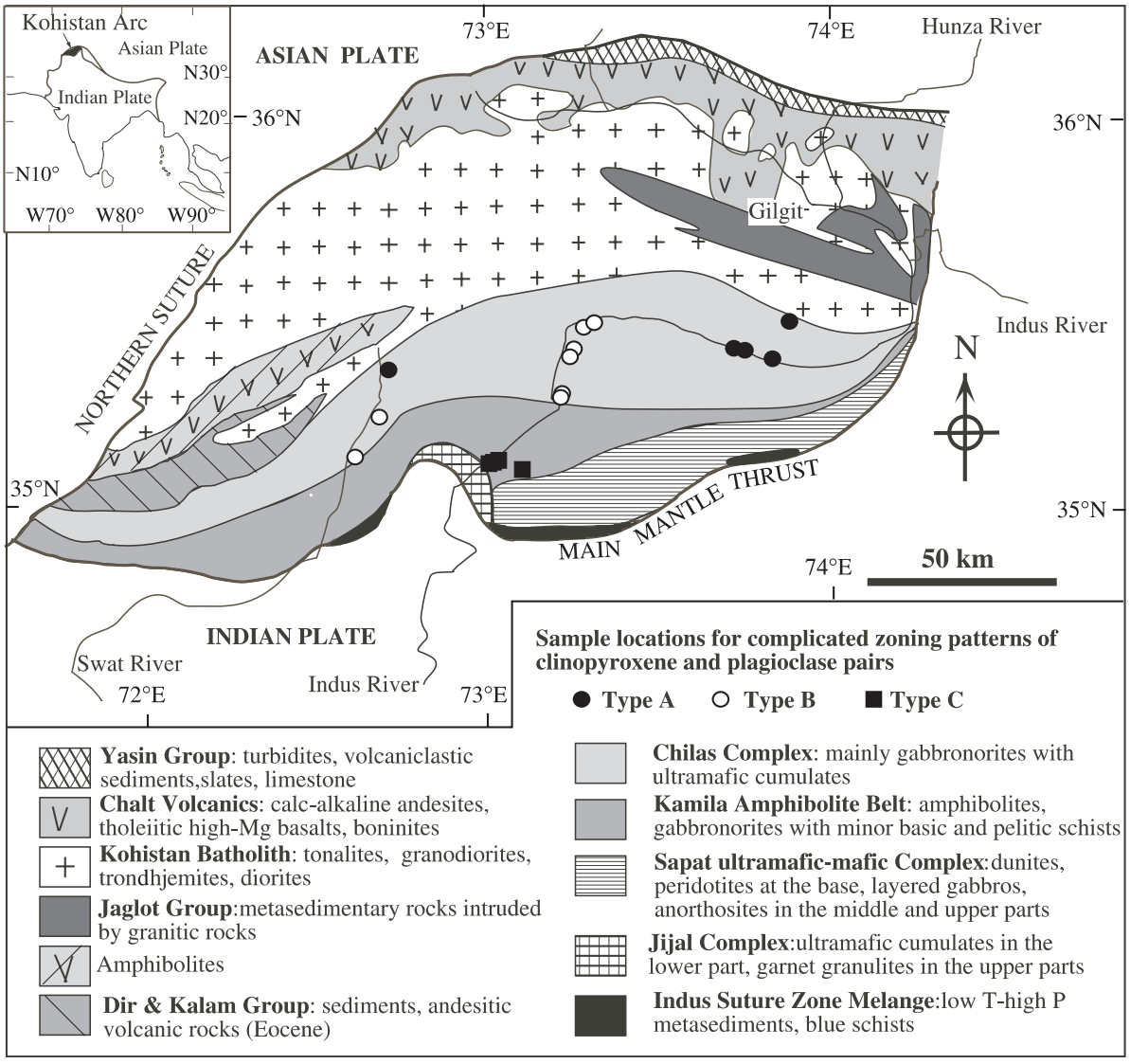


**Fig. 1.** Generalized geological map of the Kohistan Complex showing the distribution of geological units discussed in the text; modified after Treloar *et al.* (1990) and Yoshino *et al.* (1998). Inset shows the regional location of the Kohistan Complex between the Indian and Asian continents. The northern part of the Kamila Amphibolite Belt (NKA) of Yoshino *et al.* (1998) is now considered to be a part of the Chilas Complex, based on similarities of geochemistry and structure (Khan *et al.*, 1993). The NKA is treated as a southern portion of the Chilas Complex. ●, ○, ■, sample locations of rock types A, B and C, respectively (see text for details).

metamorphic $P$–$T$ conditions derived from numerous granulite terranes and xenoliths may provide general information about the perturbed continental geotherm during magmatic underplating.

The southern part of the Kohistan Arc, NW Himalayas (Fig. 1), represents levels of the crust similar to those represented by lowermost crustal mafic xenoliths. The complex might provide important clues to understanding the growth of the mafic lower crust. A regionally extensive two-pyroxene–plagioclase assemblage in metagabbros provides a means of comparing metamorphic histories by using a single geothermobarometer to avoid possible uncertainties in thermodynamic parameters. Yoshino *et al.* (1998) described prograde metamorphic $P$–$T$ paths for gabbronorites in the Kohistan Arc and emphasized the significance of magmatic accretion at mid-crustal depths. However, the physical process and thermal effects of magmatic emplacement were not discussed. In this study, additional data allow us to identify three distinct metamorphic $P$–$T$ paths from different structural levels in a single crustal sequence.

This study attempts to elucidate thermal processes in a segment of gabbroic lower crust via a comparison of metamorphic $P$–$T$ paths in Kohistan Arc metagabbros with calculated $P$–$T$ paths obtained by numerical analysis of conductive heat transfer. As one-dimensional

geodynamical models of *P–T*–time paths for regional metamorphism (England & Thompson, 1984) seem adequate to explain the key features of metamorphic *P–T* evolution, the analysis described here is restricted to a single dimension. Finally, we discuss the significance of crustal growth by magmatic accretion in light of the numerical results.

## METAMORPHIC *P–T* PATHS OF THE GABBROIC LOWER CRUST OF THE KOHISTAN ARC

### Geological setting

The Kohistan Complex is located at the boundary between the Asian and Indian plates, and has been interpreted as a Cretaceous magmatic arc (e.g. Bard, 1983; Coward *et al.*, 1986; Treloar *et al.*, 1990). There is little doubt that it includes a lower-crustal section consisting mostly of mafic rocks (Fig. 1). The northern part of the arc consists of Jurassic to Cretaceous sediments and volcanic rocks (referred to as the Yasin–Chalt and the Jaglot Groups), which are intruded by the Kohistan Batholith. The southern part of the Kohistan Complex comprises three main geological units, approximately mafic in composition; from north to south these are the Chilas Complex, the Kamila Amphibolite Belt, and the Jijal Complex (Fig. 1).

The Chilas Complex is a 300 km long, 40 km wide mafic–ultramafic body and is considered to be a thick (>10 km) stratiform intrusion (Coward *et al.*, 1986). Most of the Chilas Complex is gabbronorite of low- to medium-Fe, subalkaline affinity [enriched in large ion lithophile elements (LILE) and light rare earth elements (LREE); depleted in high field strength elements (HFSE) and heavy rare earth elements (HREE)], which locally intrudes the base of the meta-sediments and the top of meta-basalts belonging to the Kamila Amphibolite Belt (Khan *et al.*, 1993). The rest of the Chilas Complex is composed of ultramafic cumulates derived from tholeiitic picrite to high-Mg basalt parental magmas. These rocks are thought to have intruded contemporaneously based on structural relationships (Burg *et al.*, 1998). After magmatic crystallization, the gabbronorites experienced granulite-facies re-equilibration (Jan & Howie, 1980). A minimum cooling age of 70 ± 9 Ma has been obtained from a Sm–Nd isochron of a garnet-bearing granulite equilibrated at ~700°C and ~0·7 GPa in the Chilas Complex (Yamamoto, 1993; Yamamoto & Nakamura, 2000).

The Kamila Amphibolite Belt comprises mostly coarse- to medium-grained amphibolite with relict pods of gabbronorites, mafic schists and minor pelitic schists intruded by subordinate hornblendite, diorite, anorthosite, and granite (Treloar *et al.*, 1990; Khan *et al.*, 1993). Anastomosing shear zones related to the collision with the Asian plate are widely developed in the Kamila Amphibolite Belt (Treloar *et al.*, 1990; Yoshino & Okudaira, 2004). More than two-thirds of the amphibolites in the Indus Valley are metamorphosed gabbroic rocks, which have a low concentration of Ti, trace element patterns with a distinct negative anomaly of Nb relative to REE, and chondrite-normalized REE patterns similar to those of the Chilas Complex gabbronorites (Khan *et al.*, 1993). Hydration of the pyroxene granulites can be recognized by the presence of relic pyroxene rimmed by hornblende in the coarse-grained amphibolites (Yamamoto, 1993; Yoshino *et al.*, 1998). Relic pyroxene granulites are preserved as undeformed pods surrounded by foliated amphibolites. Other high-Ti amphibolites with characteristics transitional between normal and enriched mid-ocean ridge basalt (N-MORB and E-MORB) and enriched HFSE and HREE signatures, have been interpreted as remnant oceanic crust intruded by the low-Ti metabasites (Khan *et al.*, 1993).

The Jijal Complex is composed of meta-ultramafic rocks and metagabbros. The former are interpreted to be cumulates derived from an arc-related, high-Mg tholeiitic magma (Jan & Windley, 1990). Sm–Nd whole-rock–mineral isochrons from garnet-free and garnet-bearing metagabbros, which are in contact with each other in the Jijal Complex, yield ages of 91·0 ± 6·3 Ma and 118 ± 12 Ma, respectively (Yamamoto & Nakamura, 2000). The garnet-bearing and orthopyroxene-free metagabbroic rocks referred to as garnet granulites have undergone high-pressure granulite-facies metamorphism (700–950°C, >1·0 GPa) (Yamamoto, 1993; Yoshino *et al.*, 1998; Ringuette *et al.*, 1999). The estimated equilibration pressures for the Jijal Complex granulites are considerably higher than those obtained for the Chilas Complex. However, whether the Jijal Complex granulites are derived from high-pressure igneous intrusions (Ringuette *et al.*, 1999) or are high-pressure equivalents of pyroxene granulites (Jan & Howie, 1981; Yamamoto, 1993; Yoshino *et al.*, 1998) remains controversial.

### Petrography

The pyroxene granulites derived from gabbronorite protoliths used for geothermobarometry occur sporadically throughout the lower-crustal section of the Kohistan Arc, with the exception of the Jijal Complex. In the Chilas Complex, pyroxene granulites are generally preserved without evidence of retrograde hydration, but this is rare for the Kamila Amphibolite Belt rocks. Pyroxene granulites are composed of clinopyroxene, orthopyroxene and plagioclase, with minor amounts of quartz, hornblende and Fe–Ti oxides. They have various microstructures ranging from cumulate textures suggestive of

crystallization from a basaltic melt to equigranular textures indicating metamorphic recrystallization. Within the cumulate microstructures, a clinopyroxene core containing well-developed exsolution lamellae, and therefore representative of high-temperature crystallization from magma, is surrounded by an exsolution-free metamorphic clinopyroxene rim with well-preserved Al zoning. This observation suggests that the igneous clinopyroxene was overgrown during high-temperature metamorphism after crystallization from magma. In contrast, equigranular clinopyroxene grains do not contain exsolution lamellae and show little evidence for magmatic crystallization. Quartz is commonly observed as a thin film between plagioclase and clinopyroxene in garnet-free pyroxene granulites or as very small grains (1–2 μm) included within clinopyroxene rims adjacent to plagioclase. These quartz textures seem to be formed by breakdown reactions of plagioclase: anorthite = Ca Tschermaks (in clinopyroxene) + quartz and albite = jadeite (in clinopyroxene) + quartz.

Yoshino *et al.* (1998) classified zoning patterns of Al in clinopyroxene and plagioclase within the cumulate-textured pyroxene granulites of the southern Kohistan Arc into two types (types B and C). In this study, additional data from the northern Chilas Complex show another distinct type of Al zoning patterns (type A). In type A zoning (Fig. 2a), the Al content of clinopyroxene grains is almost constant in the core and decreases toward the rim. In contrast, the anorthite content in plagioclase grains increases monotonically towards the rim. Type B patterns (Fig. 2b) are characterized by complex zoning in which the Al content increases radially from the core of each clinopyroxene grain before decreasing abruptly near the rim. The anorthite content in plagioclase decreases slightly at the rim and then increases immediately adjacent to a neighboring clinopyroxene. In type C patterns (Fig. 2c), the Al content in clinopyroxene grains is almost constant in the core and increases outward from the core. The anorthite content in plagioclase at the rim exhibits a marked increase towards the outer margin. Based on the $Fe^{3+}$ contents of clinopyroxene grains (estimated by stoichiometric normalization), the interrelationships of compositional zoning between plagioclase and clinopyroxene suggest that the breakdown of a Ca-Tschermaks component ($CaAl_2SiO_6$) in clinopyroxene is responsible for types A and B, and a jadeite component ($NaAlSi_2O_6$) for type C. Rocks with type A clinopyroxene are restricted to the northern Chilas Complex, whereas type C pyroxenes occur only in the southern end of the Kamila Amphibolite Belt adjacent to the Jijal garnet granulites. Rocks containing type B clinopyroxene occur in the intervening region (Fig. 1). Peak Al contents in clinopyroxene of the pyroxene granulites increase from 1·2 to 4·6 wt % southward.

### Metamorphic *P–T* paths of mafic granulites

Aluminum zoning in plagioclase and clinopyroxene is a powerful tool for estimating the *P–T* path of rocks metamorphosed under very high temperature conditions, as the rate of intracrystalline Al diffusion is very slow. The Al zoning was measured in clinopyroxene and plagioclase from only those pyroxene granulites with preserved igneous textures, as equigranular grains do not record the earliest metamorphic *P–T* path. We assume that the growth surfaces of clinopyroxene and plagioclase were at equilibrium during metamorphism (Fig. 2). Based on this assumption and the isopleths of the two plagioclase breakdown reactions described above (Anovitz, 1991), the zoning patterns allow us to estimate the metamorphic *P–T* paths for each plagioclase–clinopyroxene pair (Fig. 3).

The results indicate that metamorphic temperatures (700–800°C) during the earliest stage were not appreciably different for the three zoning types. Peak pressures, however, range from 0·6 to 1·2 GPa. For type A samples, the metamorphic *P–T* paths are nearly isobaric cooling paths and estimated initial pressures are slightly lower (around 0·6 GPa) than those calculated for the other types. Prograde paths obtained from type B and C samples have a relatively constant $dP/dT$ slope throughout metamorphism. The data also indicate that peak temperatures (700–800°C) experienced by the different zoning types were not appreciably different, whereas peak pressures varied from 0·7 to 1·2 GPa. The pressure differences along the prograde paths are larger at lower structural levels (type C) than at higher ones (type B).

## THERMAL MODELING

### Geological constraints

In the Kohistan island arc system, continuous igneous activity might be assumed to have occurred for the duration of subduction-related magmatism. In the lower-crustal sequence, the rock assemblages indicating crustal thickening are within the structurally lower sequence (type B and C), whereas the rocks exhibiting only retrograde isobaric cooling paths lie within the uppermost part (type A). These different metamorphic *P–T* paths at different depths could be interpreted in terms of a magmatic 'intraplate model' as follows. First, basaltic magma derived from the mantle cools and crystallizes at mid-crustal depths. Second, pre-existing solidified gabbroic crust located beneath the intruding magma undergoes an increase in pressure (magma loading) and a corresponding rise in temperature as a result of conductive heat flow from the magma. This second step results in *P–T* paths characterized by an increase in pressure

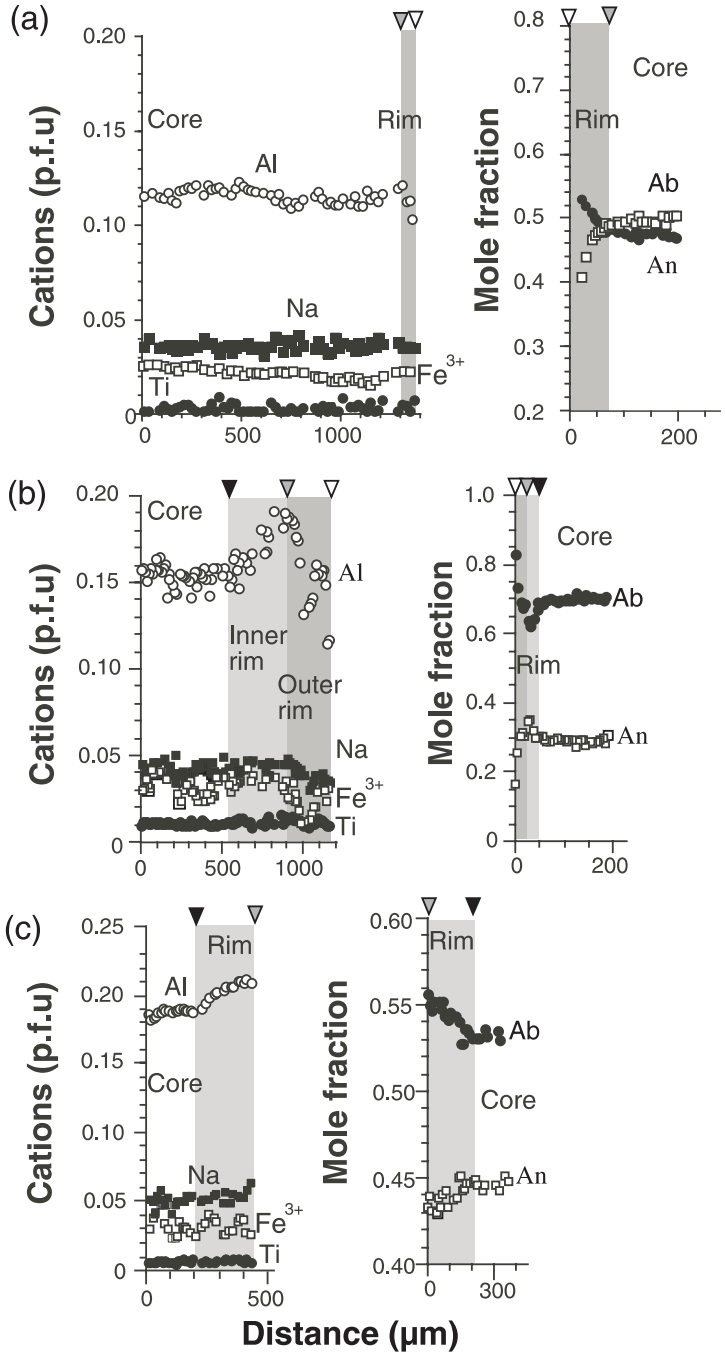


**Fig. 2.** Representative compositional zoning profiles across touching pairs of plagioclase and clinopyroxene. (a) Sample KT7 of type A. (b) Sample SM7 of type B. (c) Sample KU5 of type C. (b) and (c) are data from Yoshino *et al.* (1998). Black, grey and white arrowheads correspond to the equilibrium points between clinopyroxene and plagioclase of early, peak and later metamorphic conditions, respectively.

accompanying a relatively small increment of temperature. The basaltic lower crust consequently extends downward and thickens in response to further basaltic intrusion. Third, later intrusions undergo only cooling at near-constant depth, producing an isobaric cooling path in the upper levels of the lower crust.

In the Jijal Complex, the deeper part of the gabbronoritic body may have been metamorphosed into garnet granulite during crustal thickening (e.g. Yamamoto & Yoshino, 1998; Yoshino *et al.*, 1998). If this process occurred within the Cretaceous Kohistan Arc, then the deeper parts of the crust must be older than the shallower

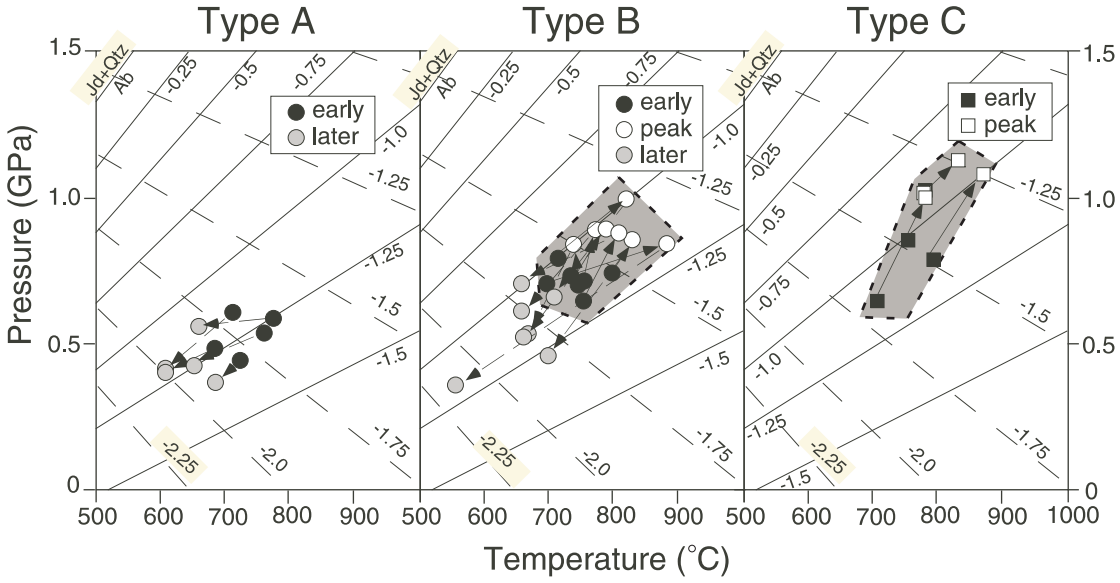


**Fig. 3.** Pressure–temperature conditions estimated from Al-zoning thermobarometry in clinopyroxene and plagioclase and representative pairs of Al zoning in both minerals for type A, type B, and type C. In general, the highest peak conditions increase towards the south. Continuous-line and dashed arrows indicate prograde and retrograde $P$–$T$ vectors for each sample, respectively. Dashed and continuous lines indicate isopleths of $\log_{10}K$ (equilibrium coefficient) derived from Anovitz (1991) for reactions albite (Ab) = jadeite (Jd) + quartz (Qtz) [$K_1 = a_{Jd}/(a_{Ab}a_{Qtz})$], and anorthite (An) = Ca-Tschermaks (CaTs) + quartz (Qtz) [$K_2 = a_{CaTs}/(a_{An}a_{Qtz})$], respectively. Activities ($a$) of clinopyroxene and plagioclase components were calculated using the procedure of Yoshino *et al.* (1998). Activity of quartz is set to unity based on the stable coexistence of quartz. Lower-pressure results include larger error because of uncertainty of activity models for clinopyroxene solid solutions. Shaded areas show the range of prograde metamorphic $P$–$T$ conditions for Kohistan granulites.

parts. The nearly 30 Myr difference in Sm–Nd isochron ages of the pyroxene granulite (118 ± 12 Ma) and garnet granulite (91 ± 6, 94 ± 5 Ma) in the Jijal Complex (Yamamoto & Nakamura, 2000) is probably equivalent to the time interval between the basaltic intrusions and the high-pressure metamorphic overprint during subsequent crustal thickening.

If the Kohistan island arc formed by subduction-related processes, then the magmatic input that formed the thickened mafic lower crust presumably occurred at approximately uniform mid-crustal depths, and therefore represents magmatic 'intraplating' rather than magmatic underplating. However, the magmatic intraplate mode poses two major problems with respect to the metamorphic evolution of the Kohistan Arc. One is the rarity of olivine–pyroxene-dominant ultramafic cumulates in the Kohistan gabbroic sequence; only a single mappable body of ultramafic cumulates is observed in the southern part of the Jijal Complex. Another problem is the preservation of high-temperature conditions (~1000°C) in the lowermost crust (Yamamoto, 1993; Ringuette *et al.*, 1999), as it is so far from the advective heat source in the mid-crust that such high temperatures could not be attained without an unusually high geothermal gradient.

The first of these issues may be explained by the fractionation of ultramafic cumulates from primitive basaltic (picritic) magmas derived from the mantle at the crust–mantle boundary (Moho). More evolved basalts that retain a distinct density contrast with respect to the solidified gabbros might ascend to mid-crustal levels (Arndt & Goldstein, 1989). In this case, magmatic accretion to the crust can take place at both mid-crustal depths and at the Moho, and supply the heat required for the high-grade metamorphism inferred to have affected the Kohistan Complex. In this manner, the gabbroic lower crust would be heated from above and below; this process is investigated below using thermal models that allow us to compare metamorphic $P$–$T$ paths.

## Simulation model

Based on geological constraints for the magmatic and metamorphic evolution of the Kohistan Arc, we have constructed a simple numerical model. As we are interested in the long-term metamorphic $P$–$T$ path of the Kohistan gabbroic crust that would result from magmatic accretion, a one-dimensional solution of the heat transfer equation provides an adequate description of the thermal structure of the crust and its variation with time. The numerical domain is composed of three layers: a tonalitic upper crust; a gabbroic lower crust; and an upper mantle with distinct thermal properties (Table 1); this configuration is typical of oceanic island arc crust (Suyehiro *et al.*, 1996). The initial condition imposed on magmatic accretion is that it occurs at a depth (10 km) equal to half the total crustal thickness (20 km). This thickness cannot be

*Table 1: Modeling parameters*

| | |
|---|---|
| Surface temperature | 0°C |
| Specific heat | |
| Upper crust | 880 J $kg^{-1}$ $m^{-1}$ |
| Lower crust | 1100 J $kg^{-1}$ $m^{-1}$ |
| Upper mantle | 1250 J $kg^{-1}$ $m^{-1}$ |
| Thermal conductivity* | |
| Upper crust | 1/(0·16 + 0·000377) W $m^{-1}$ $K^{-1}$ |
| Lower crust | 1/(0·33 + 0·000227) W $m^{-1}$ $K^{-1}$ |
| Upper mantle | 2·8 W $m^{-1}$ $K^{-1}$ |
| Density | |
| Upper crust | 2700 kg $m^{-3}$ |
| Lower crust | 2900 kg $m^{-3}$ |
| Upper mantle | 3300 kg $m^{-3}$ |
| Surface heat production | 2·60 μW $m^{-3}$ |
| Characteristic length scale | 10 km |
| Basal heat flow | 0·03 W $m^{-2}$ |
| Basalt | |
| Intrusion temperature | 1240°C |
| Liquidus temperature | 1250°C |
| Solidus temperature | 1150°C |
| Latent heat | 396000 J $K^{-1}$ |
| Primary magma | |
| Intrusion temperature | 1300°C |
| Liquidus temperature | 1350°C |
| Solidus temperature | 1250°C |
| Latent heat | 450000 J $K^{-1}$ |

*Clauser & Huenges (1995).

constrained uniquely, but the thickness of an immature arc crust is probably less than 20 km. In this study, the boundary conditions are constant temperature (0°C) at the surface, and constant mantle heat flux ($q_m$) at the bottom of the lithosphere. The thickness of the lithosphere before the intrusion of the basaltic and picritic magmas is assumed to be 35 km. The crustal geotherm immediately prior to the first intrusion of magma is also difficult to constrain as the subsequent high-temperature metamorphism has erased most of this information. Here it is set to be ~15°C/km at the onset of oceanic lithosphere subduction, after which $q_m$ is assumed to be 0·03 W/$m^2$. The intrusion rate of basaltic magma is constrained by two observations: (1) intrusions occurred throughout a 30 Myr interval, as described above; (2) the crustal thickness of the Kohistan Arc exceeds 50 km (Yamamoto, 1993; Ringuette *et al.*, 1999). The 20 km initial thickness of the crust requires that magmatic accretion provides at least an additional 30 km of thickness, implying an average accretion rate of 1 km/Myr.

We consider two possible mechanisms for magmatic intrusion, as illustrated in Fig. 4. In the magmatic intraplate model, a 1 km thick, sheet-like basaltic intrusion occurs at the initial crustal midpoint every 1 Myr at the same depth. The implicit assumption is that the basaltic magmas rise rapidly from the source region of the upper mantle and the lower crust through fractures within the lithospheric mantle without undergoing significant cooling. The solidified basaltic magma subsides by 1 km/Myr, because it is denser than the original magma, and all intrusion takes place at the initial crustal midpoint. In the magmatic double-plate model, a 1 km thick, sheet-like basaltic intrusion occurs at the initial crustal midpoint, and a 1 km thick, sheet-like picritic intrusion occurs at the base of the crust, every 1 Myr. During magmatism, the basalt intrusion depth remains constant, whereas that of the picritic magma increases by 1 km/Myr as a result of the incremental effect of the basalt above. For simplicity we use the same thickness for both the basalt daughter and picritic parent magmas, although in reality the latter must clearly be larger. Melt intrusion is modeled as a rapid magma transport along the liquid adiabat, followed by cooling at constant pressure, as magmas ascend much faster than they cool. After intrusion, the thickness of the lithosphere instantaneously inflates by 1 or 2 km in the intraplate and double-plate models, respectively.

The governing heat flow equation has been solved numerically using an explicit finite-difference method with a 1 km grid spacing and a $3{\cdot}15 \times 10^9$ s (100 yr) time step. Latent heat of crystallization is calculated by assuming the crystallization reactions to be a continuous linear function of temperature across the crystallizing interval. Recharge and convection within the magma are neglected, as are dehydration reactions in the wall rocks. The production and consumption of heat are incorporated into the numerical model using an effective heat capacity and an effective thermal diffusivity for magma undergoing crystallization.

As *P–T* paths obtained for the Kohistan Arc pertain to only part of the basaltic lower crust, we focus specifically on results from 11 km (just below the first basaltic intrusion) and 19 km (just above the Moho). Although the episodic addition of magma causes an oscillatory perturbation of the thermal structure of the adjacent layers, we neglect these oscillations and use the maximum temperature attained during each 1 Myr intrusion phase as the relevant metamorphic temperature. Finally, we also compute the metamorphic *P–T* paths of the 1 km thick basaltic body intruded 10 Myr after the onset of magmatic accretion.

## Results of the simulation

The numerical simulations clearly illustrate the large effects of magmatic accretion on the ambient crustal conditions. Figures 5 and 6 depict the evolution of the geotherm and *P–T* paths, respectively. For all magmatic underplating mechanisms, the ultimate thermal effects

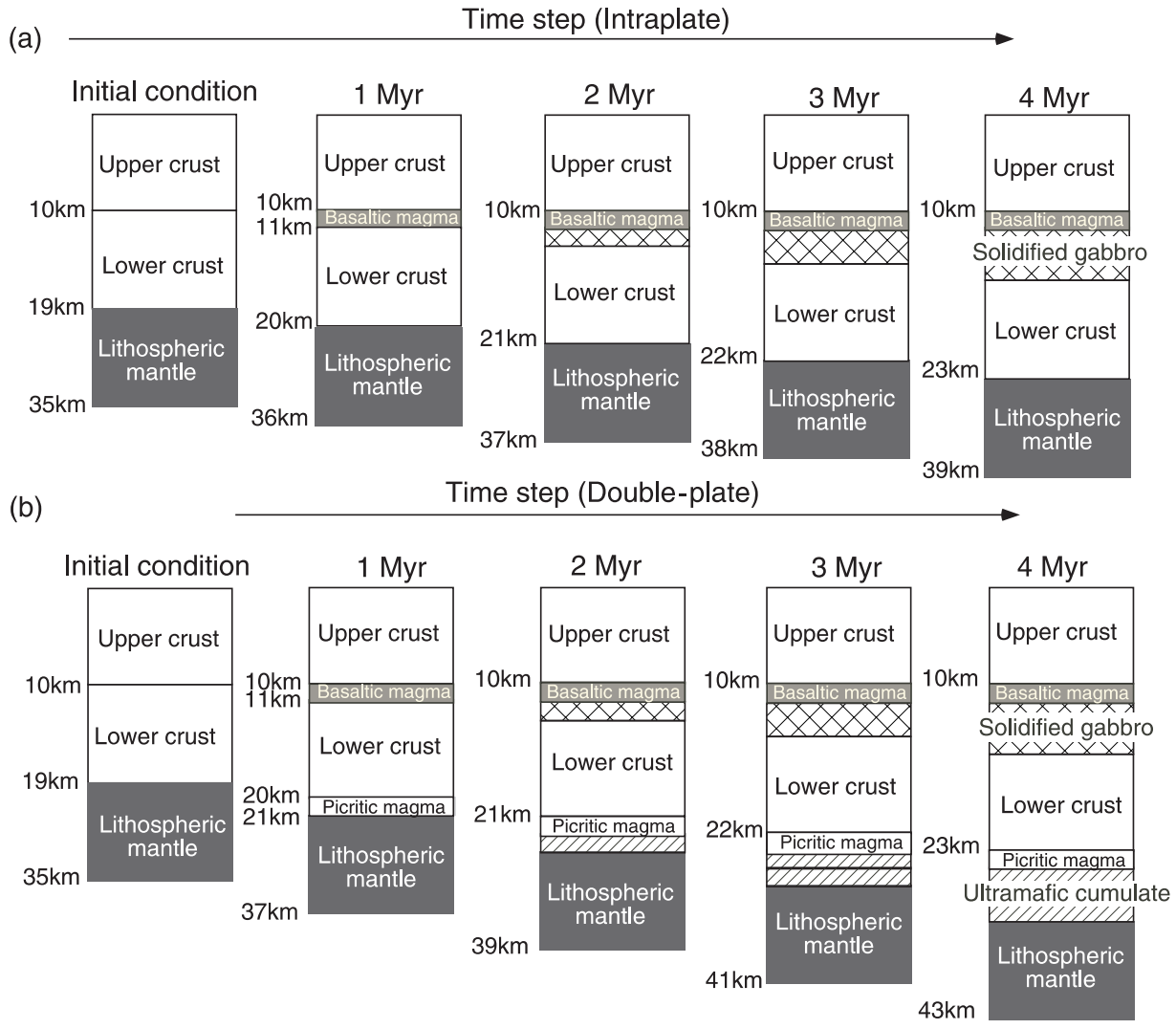


**Fig. 4.** Schematic drawing of the two magmatic accretion models. (a) and (b) show magmatic intraplate and double-plate models, respectively.

are similar. In the short term, each newly intruded layer undergoes rapid cooling following its emplacement, whereas the adjacent crust is heated by conduction and latent heat released by the crystallizing magma. In the long term, the metamorphic history of the crust is controlled by the geotherm, which approaches a steady-state configuration 5–15 Myr after the initiation of magmatism. Thereafter, the metamorphic $P$–$T$ paths have approximately the same gradient. The establishment of a steady-state geotherm in the lower crust indicates that the intrusion rate is slower than the rate of conductive heat transfer and that there are consequently no appreciable temperature maxima immediately following accretion.

In the case of the magmatic intraplate model, which involves only basaltic intrusion at 10 km and a constant basal heat flow of 0·03 W/m$^2$, the quasi-steady-state geotherm is established within 15 Myr (Fig. 5a). The d$P$/d$T$ slope of prograde metamorphic $P$–$T$ paths is nearly consistent with the paths estimated from the clinopyroxene and plagioclase Al-zoning. However, metamorphic temperatures at greater depths are distinctly lower than those estimated for the Kohistan Arc (Fig. 6a). If the basal heat flux is increased to 0·06 W/m$^2$, the geotherm matches the petrologically estimated temperatures better. However, in this case, the predicted d$P$/d$T$ slope is lower than required to match the Kohistan Complex data. Furthermore, it is unlikely that temperatures at the base of the lithospheric mantle ever exceeded 1500°C.

The thermal evolution described by the magmatic double-plate model is controlled by the two zones of transient magmatic heating. Although the distance between the picritic and basaltic intrusions increases

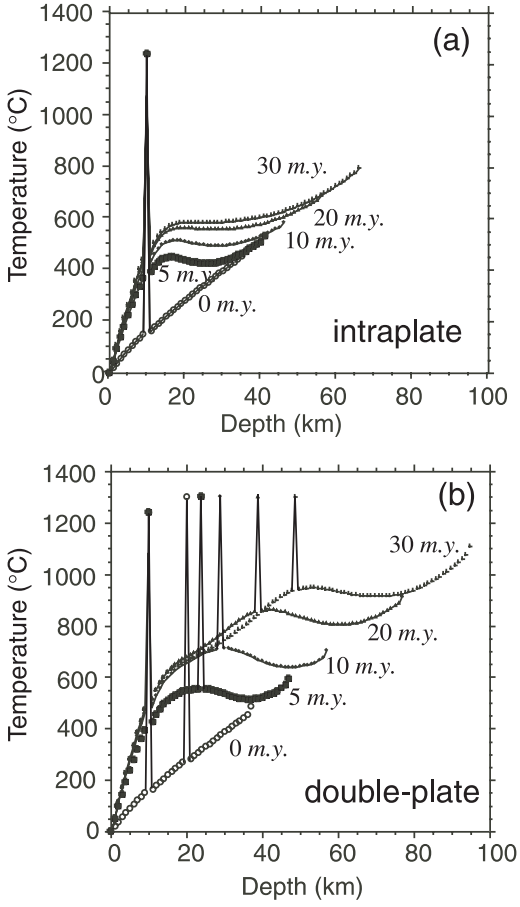


**Fig. 5.** Results of the numerical simulations. (a) and (b) show the changing thermal structure of the lithosphere with time for models of intraplate and double-plate magmatic accretion, respectively.

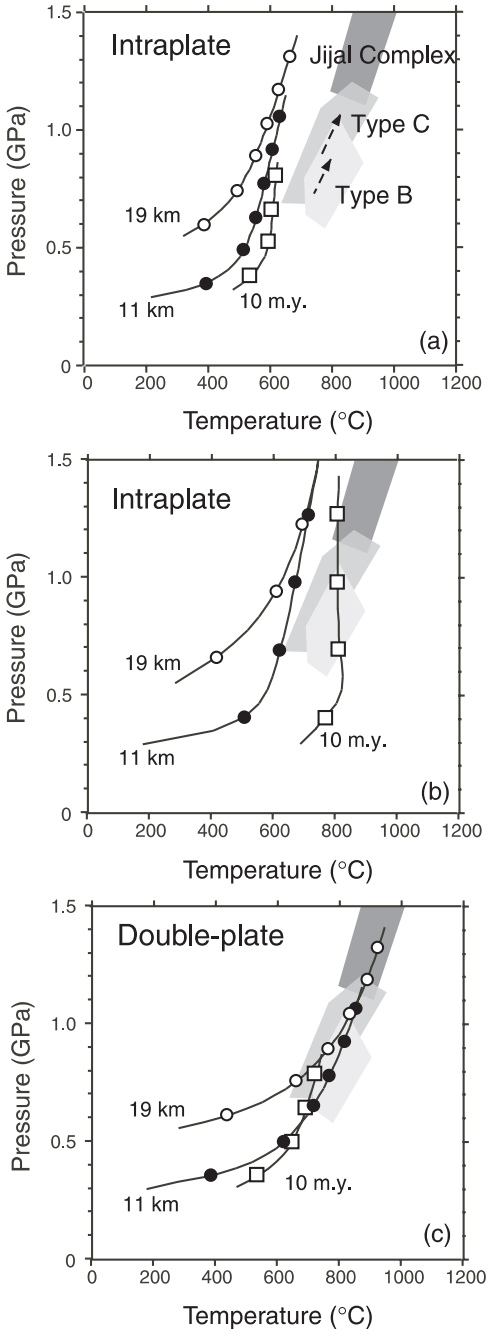


**Fig. 6.** Metamorphic *P–T* paths calculated for the two magmatic accretion models. ●, ○, calculated *P–T*–time paths at initial depths of 11 km and 19 km, respectively. □, calculated *P–T*–time paths of the body, which intruded 10 Myr after the onset of magmatic accretion. (a) and (b) illustrate calculated *P–T*–time paths (every 5 Myr) for the intraplate models with intrusion rates of 1 km/Myr and 2 km/Myr, respectively. (c) represents calculated *P–T*–time paths (every 5 Myr) for the double-plate model. Mid-gray and light gray areas represent the range of prograde metamorphic *P–T* paths for types C and B from Fig. 3. The dark gray area indicates the range of prograde metamorphic *P–T* paths for lowermost crustal levels (Jijal Complex) of the Kohistan crust (Yamamoto, 1993). Dashed arrows in (a) indicate average metamorphic *P–T* conditions of pyroxene granulites of types B and C.

monotonically with time, no appreciable cooling occurs in the intervening section of the crust during the model's entire 30 Myr duration; in particular, a quasi-steady-state geotherm develops after 10 Myr (Fig. 5b). Compared with the magmatic intraplate model, picritic intrusions at the base of the crust maintain granulite-facies conditions there in spite of an increasing distance from the source of heat caused by progressive burial of the solidified intrusions (Fig. 6c). This model can explain both the shape of the average metamorphic *P–T* paths and the absolute *P–T* conditions of the lower-crustal section in the Kohistan Arc.

The main cause of the lower-temperature conditions predicted by the intraplate model may be directly attributed to the total addition of heat, which is half that of the double-plate model. However, even if the intraplate model is calculated using the same mass flux (that is, a 2 km thick basaltic intrusion at mid-crustal depths every 1 Myr), the predicted temperatures remain lower than inferred for the Kohistan Complex (Fig. 6b) and the d*P*/d*T* slope is very different. Furthermore, the intraplate

model is deemed unlikely because the thickness of mafic lower crust accreted at this rate is too large. Therefore, we favor the double-plate model for explaining both the shape of the $P$–$T$ paths and the range of $P$–$T$ conditions of the lower crust of the Kohistan Complex.

## DISCUSSION

### Evaluation of the model

Several assumptions made in constructing our numerical model affect its results, such as those concerning the initial geotherm, intrusion rate, lithological structure of the crust, the second-order thermal effects of fractionated magmas and water content in magmas. If the arc crust developed on top of an oceanic crust via magmatic accretion, then the initial geotherm used here may have been too low. However, this effect is likely to be small, as we observe the development of an almost steady-state geotherm within 10 Myr of the intrusion commencing.

Unfortunately, the intrusion rate cannot be evaluated directly by using the age data, because there are large errors on the age determination. When the intrusion rate is set to be 1 km/Myr, the volumetric growth rate is 50–100 $km^3$/km arc strike length per Myr, assuming a width of 50–100 km for the Kohistan Arc (see Fig. 1). This volumetric rate is consistent with the recent estimated growth rates for the Izu–Bonin island arc of 80–200 $km^3$/km per Myr (Arculus, 1999) and for various island arcs of 30–95 $km^3$/km per Myr based on seismic and gravity data (Dimalanta *et al.*, 2002). Therefore, the intrusion rate of 1 km/Myr used in this study may be appropriate for island arc settings. In fact, if the intrusion rate were half the value used here, then the resulting geothermal gradient is so low that temperatures at lower-crustal levels do not reach granulite-facies levels in either model. In contrast, an intrusion rate twice that used here (2 km/Myr) produces an implausibly high $dP/dT$ slope for the intraplate model or leads to complete crustal melting in the case of the double-plate model.

The Kohistan island arc, which developed on top of pre-existing oceanic crust, formed an intermediate composition mid-crust during magma-driven crustal growth. Consequently, the basaltic intrusion depth is presumed to have deepened continuously, as did that of the picritic magma. Based on the peak pressure conditions estimated for the shallowest (type A) and deepest sections (type C) of the gabbroic lower crust, the final thickness of gabbroic lower crust ($\sim$30 km) is significantly greater than that of the upper crust ($<$15 km). This suggests that crustal generation rates in the middle crust may be smaller than in the lower crust, and that the distance between the depths of basaltic and picritic intrusion therefore also increased during the course of the magmatism. This process would lead to a shift of the quasi-steady-state lower-crustal geotherm towards higher temperatures.

Fractionation of picritic magma at the crust–mantle boundary may also have affected the thermal evolution of the lowermost crust. Because any residual magma probably had a higher solidus temperature owing to its approach to a cumulate composition, it will solidify faster than the picritic magma. Therefore, the present model will overestimate the effects of latent heat near the crust–mantle boundary. The process will shift the geotherm and $P$–$T$ paths towards lower temperatures than illustrated above. Consequently, given that the effects described in this and the previous paragraph are somewhat compensatory, the results of the magmatic double-plate model may be plausible.

In a magmatic arc setting, the presence of water in the mantle wedge will lower the solidus temperature of peridotite in the source region of the arc magmas (e.g. Hirose & Kawamoto, 1995). If the intrusion temperatures of picritic and basaltic magmas are lower than that of anhydrous magma by 50–100°C, the geotherm and $P$–$T$ paths are shifted towards lower temperatures than the results assuming anhydrous primary magmas. However, in the Kohistan Arc, water contents in primary magma may be small, as discussed below.

### Physical process of magmatic accretion

The depth of magmatic accretion is influenced by density variations within (e.g. Stolper & Walker, 1980) or mechanical behavior of the lithosphere (e.g. Shaw, 1980; Putirka, 1997). The gravitational equilibrium implied by the contrast in density between the crystalline host rocks and the basaltic magma is a possible mechanism for intraplating (Herzberg *et al.*, 1983). Density variations with pressure (or equivalently, with depth) are shown for some common magmas and rocks in Fig. 7. Because melts are generally less compressible than crystalline rocks of the same bulk chemistry, crystallized mafic rocks at lower-crustal depths (over 20 km) are much denser than the basaltic magma from which they solidified. Therefore, basaltic magma can ascend as a consequence of its relatively low density to a depth at which it attains neutral buoyancy with respect to the surrounding rocks. If the crust within an arc is stratified by density, such a depth might correspond to the boundary between the lower crust and low-density upper crust. This depth is approximately 15 km for the case of basaltic magma rising into an upper crust whose average density is 2750 $kg/m^3$ (representative of a granodiorite), and at this point the magma ascent will stall and the magma crystallize (see Fig. 7). When basaltic magma ponds at a point of neutral buoyancy, it tends to form a horizontal sheet. Because the Chilas Complex is overlain by the granodioritic Kohistan batholith, the boundary between them may have been the site of continuous basalt (gabbronorite) intrusion.

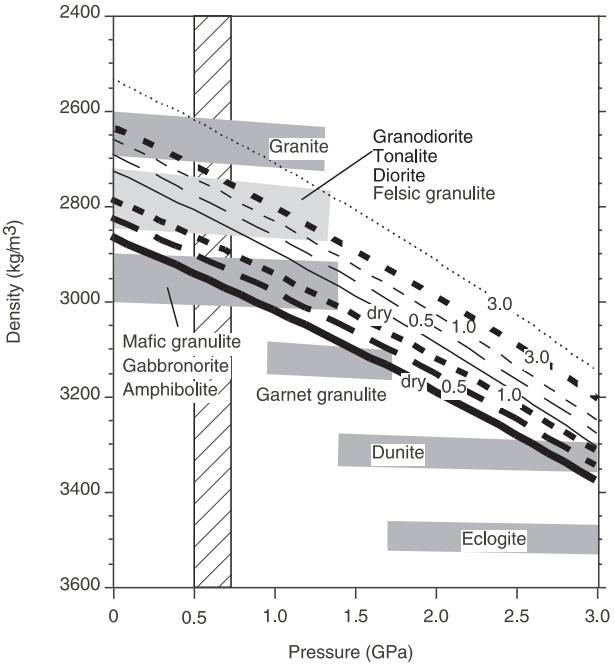


**Fig. 7.** Density–pressure relations between melts and crustal components. Shaded bands and bold lines are densities of rocks and magma, respectively. Rock density was obtained from data on various lithologies under high geothermal gradients based on the compilation of Christensen & Mooney (1995). Magma density was calculated using the partial molar volume data of Lange & Carmichael (1990) for silicate liquids and Ochs & Lange (1999) for $H_2O$. Bold and fine curves indicate depth–density relation along the adiabat for representative picritic and basaltic melts, respectively. Numbers represent water content in the melts (in wt %). Left hatched area shows depth of basaltic intrusions inferred from metamorphic *P–T* paths of this study.

However, magma genesis above subduction zones is fundamentally different from that occurring at mid-ocean ridges and in intracontinental settings, as a result of the presence of $H_2O$ derived from the dehydrating subducted slab, and the presence of refractory mantle sources in the mantle wedge above the subducting slab (e.g. Gill, 1981; Tatsumi & Eggins, 1995; Iwamori, 1998). Therefore, we must consider the effect of water in magma on the density–depth relation between rocks and melts. Water content in magma significantly affects its melt density as a result of the low molecular weight of $H_2O$ as compared with the average molecular weight of magmatic liquids. For basaltic and picritic liquids, the effect of adding 3 wt % $H_2O$ is to decrease its liquid density by 6–7% and 7–8%, respectively, using the partial molar volume data of Lange & Carmichael (1990) for silicate liquids and Ochs & Lange (1999) for $H_2O$. Using these hydrous compositions changes the level at which they are likely to intrude the crust (Fig. 7). A lower-density hydrous magma could not be trapped at lower- or mid-crustal depths and instead would ascend towards the surface until it reached its solidus, at which point it would start to degas. In contrast, if the $H_2O$ content of the magma is <1 wt %, the density–depth assumptions of the model may be appropriate, as the decrease in density is relatively small ($< \sim 2\%$).

Another possible mechanism of intraplating is related to the mechanical behavior of the lithosphere at the brittle–ductile transition zone (Putirka, 1997). Basaltic magma may be transported by fracture mechanisms through a brittle lithosphere. When stress concentrated at crack tips ($K$: stress intensity factor) exceeds a critical value ($K_c$: fracture toughness), dike propagation occurs. A transition from brittle to ductile behavior will cause an increase in $K_c$ (Scholtz, 1990). At depths greater than the elastic thickness of the lithosphere (corresponding to the depth of the brittle–ductile transition zone), dikes stall or propagate laterally. Regional variations in the cut-off depth of seismicity in SW Japan range from 10 to 20 km, although the thickness of the seismogenic layer is closely related to the strength of the crust and its thermal structure (Ito, 1997). The depths to the top of the reflective lower crust lies several kilometers below the cut-off depth of seismicity. If the reflective lower crust represents magmatic accretion at mid-crustal depths, this mechanism may play a significant role in the emplacement of basaltic magma in the mid-crust in island arc settings. If this mechanism applies to our model, the intrusion depth would initially shift to shallower depths because of an increase in the geotherm due to the intrusion of basaltic magma.

Anhydrous picritic magmas might not ascend into a thick crust because of the high density of picrite, based on density–depth relations (Fig. 7). Both picritic and olivine tholeiitic melts are expected to rise within the mantle in response to buoyancy forces, and then disperse laterally at the base of the crust. Glass inclusions in primitive arc magmas have average $H_2O$ concentrations of 1·6–1·7 wt % (Sovolev & Chaussidon, 1996). Boninites, which are an important hydrous end-member of subduction zone magmas, have higher $H_2O$ contents in the primary melts ($\sim$2 wt %) (Sovolev & Danyushevsky, 1994; Falloon & Danyushevsky, 2000). The higher $H_2O$ contents in high-alumina basalts range up to 6 wt % (Sisson & Grove, 1993). Although the amounts of $H_2O$ in the primary magmas of the Kohistan Arc are unknown, the presence of ultramafic cumulates (dunite, harzburgite and wehrlite) in the Jijal and Chilas Complexes indicates that the primary magmas intruding the lower-crustal rocks had picritic to high-Mg tholeiitic basalt compositions (Jan & Windley, 1990; Khan *et al.*, 1993). The low abundance of hornblende (hydrous) gabbros in the lower crust of the Kohistan Arc suggests that the water content in the parental basaltic magmas may have been small. In some modern island arcs only small amounts of $H_2O$ (0·2 wt %) appear to be required to generate basaltic parental magmas in the mantle wedge

based on petrological and seismological data (e.g. Kushiro, 1987).

A rough estimate of the density contrast between picritic magma with 1 wt % $H_2O$ and gabbroic rocks (Fig. 7) suggests that picritic magmas will accumulate at the crust–mantle boundary whenever the crustal thickness exceeds 30 km. Because this thickness is greater than that of normal island arcs, most modern magmatic arcs are unlikely to undergo the process of picritic underplating at the Moho. Therefore, another mechanism is required to explain the horizontal intrusion of picritic magma at the Moho. If we consider a long intrusion interval, and assume that the ratio of the upper-mantle viscosity ($\eta_m$) to the lower-crust viscosity ($\eta_{lc}$) exceeds unity (likely given the plagioclase-dominant and olivine-dominant rheologies of the lower crust and lithospheric mantle, respectively), then the Moho is a significant rheological boundary that is likely to facilitate horizontal intrusion (Parsons *et al.*, 1992). Therefore, a large viscosity contrast at the Moho probably leads to the horizontal intrusion of picritic magma at the crust–mantle boundary. Consequently, our model assuming intrusion of primary magma at the Moho can apply to the cases whether either the $H_2O$ content of the primary magma is small or the rheological contrast at the Moho is high.

## Evidence of emplacement of primary magma at the Moho

In the magmatic double-plate model presented here, fractional crystallization is assumed to be the dominant process by which primary melts evolve towards basaltic compositions at the Moho. The liquidus olivine and pyroxene fractionated from these picrites would presumably accumulate at the Moho, rather than within the crust, and further fractionation of either picrite or olivine tholeiite would yield ultramafic cumulates. The ultramafic rocks in the Jijal Complex have been considered to be cumulates derived from an arc-related, high-Mg tholeiitic magma (Jan & Windley, 1990). Ultramafic xenoliths have been found in volcanoes on Adak Island and used both to model igneous fractionation trends of low- to medium-Fe, subalkaline rocks and as evidence for crystallization of ultramafic cumulates at the Moho (Conrad & Kay, 1984; Kay & Kay, 1985; DeBari *et al.*, 1987). Although many of the granulite terranes are not associated with a large mass of ultramafic cumulate rocks because of the mechanical difficulty in exhuming large volumes of high-density ultramafic rocks, those in association with deep-seated layered gabbros at the base of a magmatic arc sequence have been reported from the Tonsina ultramafic–mafic assemblage, Alaska (DeBari & Coleman, 1989) and the Tinaquillo massif, Venezuela (Seyler *et al.*, 1998).

In addition, there is indirect evidence that primary magmas stall at the Moho. It has been suggested that scapolites in garnet granulites from the Jijal Complex were formed by infiltration of $CO_2$-rich fluids derived from decarbonation of carbonate-bearing sediments in the subducting slab (Yoshino & Satish-Kumar, 2001). As the solubility of $CO_2$ in tholeiitic basalts rapidly decreases with decreasing pressure from over 1·7 wt % at 1·5–3·0 GPa to 0·1 wt % at 1·0–1·5 GPa (Spera & Bergman, 1980), $CO_2$ would degas from tholeiitic magma near the crust–mantle boundary and infiltrate upwards to form scapolite in the lower crust. In fact, scapolite is an important constituent of mafic xenoliths in basaltic lavas and kimberlites (e.g. Lovering & White, 1964; Markwick & Downes, 2000; Sachs & Hansteen, 2000) and of mafic granulites and anorthosites (e.g. Blattner & Black, 1980; Coolen 1982).

## Applications of the magmatic accretion model

### *Granulite* P–T *conditions*

Harley (1989) and Bohlen & Mezger (1989) summarized peak metamorphic $P$–$T$ conditions of world-wide granulite terranes. Assuming that these metamorphic peak $P$–$T$ conditions represent perturbed continental geotherms during the period of granulite formation, then the geothermal gradients at shallow depths will be rather high ($\sim$50°C/km), whereas those at deeper crustal levels (>0·5 GPa) are fairly low ($\sim$10°C/km) (Fig. 8). The geotherm calculated by the magmatic double-plate model is consistent with the above data. The change of $dP/dT$ slope at mid-crustal depths can be explained by the thermal effects derived from two heat budgets.

First, accretion of basaltic magma at mid-crustal depth could maintain a supply of heat at that depth, even if the basaltic lower crust becomes abnormally thick. As a high geotherm at mid-crustal depths is maintained for the duration of magmatism, the high-temperature condition at mid-crustal depths would cause granulite-facies metamorphism as observed in most granulite terranes at a constant depth ($\sim$20 km) (Bohlen & Mezger, 1989). For example, some terranes such as the Adirondacks (Bohlen *et al.*, 1985), southern Calabria (Graessner *et al.*, 2000) and the Musgrave Block (Ellis & Maboko, 1992; White *et al.*, 2002), exhibit intermediate- to high-pressure granulite-facies metamorphism with isobaric cooling. The lowest pressures obtained from these areas are similar to pressures estimated from the Chilas Complex. In addition, when the solidus of the intruded basaltic magma exceeds the solidus of the crustal host, large-scale melting of the felsic crust above the trapping level may occur, leading to generation of granitic magma and the development of a density-stratified upper crust (e.g. Huppert & Sparks, 1988; Bergantz, 1989; Petford & Gallagher, 2001; Annen & Sparks, 2002).

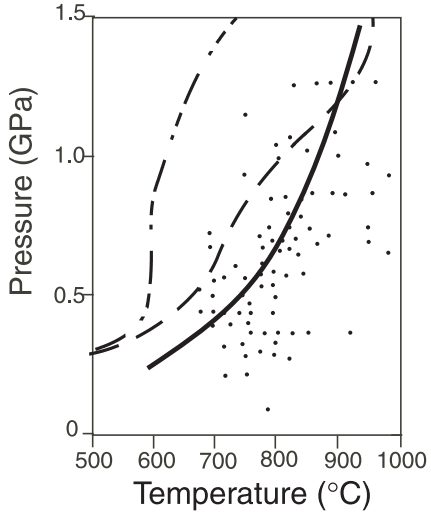


**Fig. 8.** Comparison between *P–T* conditions of crustal granulite terranes and calculated thermal structures. Dash–dotted and dashed lines indicate the thermal structure of the lithosphere after 30 Myr for the models of intraplate and double-plate accretion, respectively. Dots are *P–T* conditions for granulite terranes (Harley, 1989). Continuous line represents the average geothermal gradient during the period of granulite formation.

On the other hand, accretion of primitive magma at the Moho could maintain high-temperature conditions (~1000°C) at the base of the crust (Yamamoto, 1993; Ringuette *et al.*, 1999). Such mafic granulites (garnet granulite) with high equilibration temperatures (800–1000°C) and pressures (1–1·5 GPa) have been reported for granulite xenoliths all over the world; for example, in the Baltic Shield (Kempton *et al.*, 1995; Markwick & Downes, 2000), eastern Finland (Hölttä *et al.*, 2000), the West African craton (Toft *et al.*, 1989), at the margin of the Kaapvaal craton in South Africa and Lesotho (Griffin *et al.*, 1979; Pearson *et al.*, 1995) and the eastern margin of Australia (Griffin *et al.*, 1990). In the case of the magmatic intraplate model, the lowermost crust far from the heat sources at mid-crustal depth cannot attain such high-temperature conditions except for a condition of unusually high basal heat flux.

### *Implications for lower-crustal geochemistry*

Garnet-bearing deep crustal xenoliths are typically enriched in Eu, indicating the presence of cumulate plagioclase in their original protolith (Taylor & McLennan, 1985). Thus, the Eu enrichment took place prior to formation of the garnet granulite and not during the crystallization of garnet from a magma. The rarity of Lu/Hf enrichment in garnet-bearing lower-crustal xenoliths also suggests that garnet is not widespread in the lower-crustal protolith (Vervooft *et al.*, 2000). These geochemical characteristics are consistent with the lack of significant HREE enrichment (which would indicate garnet in the original protolith) in the vast majority of lower-crustal xenoliths (GERM, Geochemical Earth Reference Model, available at http://www.earthref.org/germ/). Therefore, most of the lower crust need not have formed by intracrustal melting at depths where garnet fractionation was occurring, but instead might have conceivably been generated at mid-crustal depths. The geochemical evidence suggests that the garnet granulites within crustal granulite xenolith suites are of metamorphic origin caused by crustal thickening, and that plagioclase fractionation probably occurs within the mid-crust.

Magmatic accretion at mid-crustal depth may facilitate the voluminous generation of eclogite as a result of mid-crustal magma loading, with the characteristics of an evolved basaltic composition such as slight enrichment in LREE. Formation of eclogite in the lower crust might lead to the delamination of this crustal component (Ringwood & Green, 1967; Kay & Kay, 1991, 1993) owing to its high density relative to the underlying lithospheric mantle (Fig. 7). The continental lithospheric mantle has been postulated to be a mantle reservoir enriched in incompatible elements (McDonough, 1990). Because the basaltic lower continental crust has significantly higher abundances of incompatible trace elements compared with oceanic crust (Rudnick & Fountain, 1995), eclogite delamination may be a mechanism by which significant amounts of incompatible trace elements are lost from the magmatically thickened crust by removal of the lowermost crust.

## CONCLUSIONS

The prograde *P–T* paths of relic two-pyroxene granulites represent a crustal thickening process within the Kohistan Arc during early to middle Cretaceous time. The first-order agreement between the inferred and calculated thermal structure and predicted metamorphic *P–T* paths supports a magmatic double-plate model, in which magmatic accretion occurs simultaneously within the mid-crust and at the crust–mantle boundary. A magmatic intraplate model does not adequately explain the metamorphic *P–T* conditions estimated from pyroxene granulites of the Kohistan Arc unless a high mantle heat flux is incorporated into the model as a boundary condition. The effect of higher basal heat flow is to alter the shape of the averaged metamorphic *P–T* paths so that they do not agree with the petrological data. In contrast, the magmatic double-plate model can explain both the shape of the metamorphic *P–T* paths and the absolute metamorphic conditions. The calculated geotherms are consistent with an array of peak granulite *P–T* conditions based on data from exposed granulite terranes and mafic granulite xenoliths. This suggests that granulite formation generally results from simultaneous intrusion of primary

magma at the crust–mantle boundary and fractionated basaltic magma at mid-crustal depths.

## ACKNOWLEDGEMENTS

The manuscript benefited from discussions with M. Toriumi and G. Kimura. An early version of the manuscript was improved by critical comments from R. J. Arculus, N. T. Arndt and E. J. Essene. Electron microprobe work was carried out in the Geological Institute, University of Tokyo, with the helpful assistance of H. Yoshida. This manuscript was improved by constructive reviews from D. J. Ellis and R. J. Arculus.

## REFERENCES

Annen, C. & Sparks, R. S. J. (2002). Effects of repetitive emplacement of basaltic intrusions on thermal evolution and melt generation in the crust. *Earth and Planetary Science Letters* **203**, 937–955.

Anovitz, L. M. (1991). Al zoning in pyroxene and plagioclase: window on late prograde to early retrograde *P–T* paths in granulite terranes. *American Mineralogist* **76**, 1328–1343.

Arculus, R. J. (1999). Origins of the continental crust. *Journal and Proceedings of the Royal Society of New South Wales* **132**, 83–110.

Arndt, N. T. & Goldstein, S. L. (1989). An open boundary between lower continental crust and mantle: its role in crust formation and crustal recycling. *Tectonophysics* **161**, 201–212.

Bard, J. P. (1983). Metamorphism of an obducted island arc: example of the Kohistan sequence (Pakistan) in the Himalayan collided range. *Earth and Planetary Science Letters* **65**, 133–144.

Bergantz, G. W. (1989). Underplating and partial melting: implications for melt generation and extraction. *Science* **245**, 1093–1095.

Blattner, P. & Black, P. M. (1980). Apatite and scapolite as petrogenetic indicators in granulites of Milford Sound, New Zealand. *Contributions to Mineralogy and Petrology* **74**, 339–348.

Bohlen, S. R. & Mezger, K. (1989). Origin of granulite terranes and the formation of the lowermost continental crust. *Science* **244**, 326–329.

Bohlen, S. R., Valley, J. W. & Essene, E. J. (1985). Metamorphism in Adirondacks I. Petrology, pressure and temperature. *Journal of Petrology* **26**, 971–992.

Burg, J. P., Bodinier, J. L., Chaudhry, S., Hussain, S. & Dawood, H. (1998). Infra-arc mantle transition and intra-arc mantle diapirs in the Kohistan Complex (Pakistani Himalaya): petro-structural evidence. *Terra Nova* **10**, 74–80.

Christensen, N. I. & Mooney, W. D. (1995). Seismic velocity structure and composition of the continental crust: a global view. *Journal of Geophysical Research* **100**, 9761–9788.

Clauser, C. & Huenges, E. (1995). Thermal conductivity of rocks and minerals. In: Ahrens, T. J. (ed.) *Rock Physics and Phase Relations: a Handbook of Physical Constants*. Washington, DC: American Geophysical Union, pp. 105–126.

Conrad, W. K. & Kay, R. W. (1984). Ultramafic and mafic intrusions from Adak Island: crystallization history and implications for the nature of primary magmas and crustal evolution in the Aleutian arc. *Journal of Petrology* **25**, 88–125.

Coolen, J. J. M. M. M. (1982). Carbonic fluid inclusions in granulites from Tanzania—a comparison of geobarometric methods based on fluid density and mineral chemistry. *Chemical Geology* **37**, 59–77.

Coward, M. P., Broughton, R. D., Luff, I. W., Petterson, M. G., Pudsey, C. J., Rex, D. C. & Khan, M. A. (1986). Collision tectonics in the NW Himalayas. In: Coward, M. P. & Ries, A. C. (eds) *Collision Tectonics*. Oxford: Blackwell, pp. 203–219.

DeBari, S. M. & Coleman, R. G. (1989). Examination of the deep levels of an island arc: evidence from the Tonsina ultramafic–mafic assemblage, Tonsina, Alaska. *Journal of Geophysical Research* **94**, 4373–4391.

DeBari, S. M., Kay, S. M. & Kay, R. W. (1987). Ultramafic xenoliths from Adagdak volcano, Adak, Aleutian Islands, Alaska: deformed igneous cumulates from the Moho of an island arc. *Journal of Geology* **95**, 329–341.

Dimalanta, C., Taira, A., Yumul, G. P., Jr, Tokuyama, H. & Mochizuki, K. (2002). New rates of western Pacific island arc magmatism from seismic and gravity data. *Earth and Planetary Science Letters* **202**, 105–115.

Ellis, D. J. & Maboko, M. A. H. (1992). Precambrian tectonics and the physicochemical evolution of the continental crust 1. The gabbro–eclogite transition revisited. *Precambrian Research* **55**, 491–506.

England, P. C. & Thompson, A. B. (1984). Pressure–temperature–time paths of regional metamorphism. Part I: Heat transfer during the evolution of regions of thickened continental crust. *Journal of Petrology* **25**, 894–928.

Falloon, T. J. & Danyushevsky, L. V. (2000). Melting of refractory mantle at 1·5, 2 and 2·5 GPa under anhydrous and $H_2O$-undersaturated conditions: implications for the petrogenesis of high Ca-boninites and the influence of subduction components on mantle melting. *Journal of Petrology* **41**, 257–283.

Fountain, D. M. & Salisbury, M. H. (1981). Exposed cross-sections through continental crust: implications for crustal structure, petrology and evolution. *Earth and Planetary Science Letters* **56**, 263–277.

Gill, J. B. (1981). *Orogenic Andesites and Plate Tectonics*. New York: Springer.

Graessner, T., Schenk, V., Bröcker, M. & Mezger, K. (2000). Geochronological constraints on the timing of granitoid magmatism, metamorphism and post-metamorphic cooling in the Hercynian crustal cross-section of Calabria. *Journal of Metamorphic Geology* **18**, 409–421.

Griffin, W. L., Carswell, D. A. & Nixon, P. H. (1979). Lower crustal granulites and eclogites from Lesotho, Southern Africa. In: Boyd, F. R. & Meyer, H. O. A. (eds) *The Mantle Sample*. Washington, DC: American Geophysical Union, pp. 59–86.

Griffin, W. L., O'Reilly, S. Y. & Pearson, N. J. (1990). Eclogite stability near the crust–mantle boundary. In: Carswell, D. A. (ed.) *Eclogites and Related Rocks*. Glasgow: Blackie, pp. 291–314.

Harley, S. L. (1989). The origin of granulites: a metamorphic perspective. *Geological Magazine* **126**, 215–247.

Herzberg, C. T., Fyfe, W. F. & Carr, M. J. (1983). Density constraints on the formation of the continental Moho and crust. *Contributions to Mineralogy and Petrology* **84**, 1–5.

Hirose, K. & Kawamoto, T. (1995). Hydrous partial melting of lherzolite at 1 GPa: the effect of $H_2O$ on the genesis of basaltic magmas. *Earth and Planetary Science Letters* **133**, 463–473.

Holbrook, W. S., Mooney, W. D. & Christensen, N. I. (1992). The seismic velocity structure of the deep continental crust. In: Fountain, D. M., Arculus, R. & Kay, R. W. (eds) *Continental Lower Crust*. Amsterdam: Elsevier, pp. 1–44.

Hölttä, P., Huhma, H., Mänttäri, I., Peltonen, P. & Juhanoja, J. (2000). Petrology and geochemistry of mafic granulite xenoliths from the Lahtojoki kimberlite pipe, eastern Finland. *Lithos* **51**, 109–134.

Huppert, H. E. & Sparks, R. S. J. (1988). The generation of granitic magmas by intrusion of basalt into continental crust. *Journal of Petrology* **29**, 599–624.

Ito, K. (1997). Seismogenic layer, reflective lower crust, surface heat flow and large inland earthquakes. *Tectonophysics* **306**, 423–433.

Iwamori, H. (1998). Transportation of $H_2O$ and melting in subduction zones. *Earth and Planetary Science Letters* **160**, 65–80.

Jan, M. Q. & Howie, R. A. (1980). Ortho- and clinopyroxenes from pyroxene granulites of Swat Kohistan, northern Pakistan. *Mineral Magazine* **43**, 715–728.

Jan, M. Q. & Howie, R. A. (1981). The mineralogy and geochemistry of the metamorphosed basic and ultrabasic rocks of the Jijal complex, Kohistan, NW Pakistan. *Journal of Petrology* **22**, 85–126.

Jan, M. Q. & Windley, B. F. (1990). Chromian spinel–silicate chemistry in ultramafic rocks of the Jijal Complex, northwest Pakistan. *Journal of Petrology* **31**, 667–715.

Kay, R. W. & Kay, S. M. (1985). Role of crystal cumulates and the oceanic crust in the formation of the lower crust of the Aleutian arc. *Geology* **13**, 461–464.

Kay, R. W. & Kay, S. M. (1991). Creation and destruction of lower continental crust. *Geological Rundschau* **80**, 259–278.

Kay, R. W. & Kay, S. M. (1993). Delamination and delamination magmatism. *Tectonophysics* **219**, 177–189.

Kempton, P. D., Downes, H., Sharkov, E. V., *et al.* (1995). Petrology and geochemistry of xenoliths from the Northern Baltic shield: evidence for partial melting and metasomatism in the lower crust beneath an Archaean terrane. *Lithos* **36**, 157–184.

Khan, M. A., Jan, M. Q. & Weaver, B. L. (1993). Evolution of the lower arc crust in Kohistan: temporal arc magmatism through early, mature and intra-arc rift stages. In: Malinconico, L. L. & Lillie, J. (eds) *Tectonics of the Western Himalayas. Geological Society, London, Special Publications* **74**, 123–138.

Kushiro, I. (1987). A petrological model for the mantle wedge and lower crust of the Japanese island arcs. In: Mysen, B. O. (ed.) *Magmatic Processes: Physicochemical Principles. Geochemical Society Special Publications* 165–181.

Lange, R. L. & Carmichael, I. S. E. (1990). Thermodynamic properties of silicate liquids with emphasis of density, thermal expansion and compressibility. In: Nicholls, J. & Russell, J. K. (eds) *Modern Methods of Igneous Petrology: Understanding Magmatic Processes. Mineralogical Society of America, Reviews in Mineralogy* **24**, 25–64.

Lovering, J. F. & White, A. J. R. (1964). The significance of primary scapolite in granulitic inclusions from deep-seated pipes. *Journal of Petrology* **5**, 195–218.

Markwick, A. J. W. & Downes, H. (2000). Lower crustal granulite xenoliths from the Arkhangelsk kimberlite pipes: petrological, geochemical and geophysical results. *Lithos* **51**, 135–151.

McDonough, W. F. (1990). Constraints on the composition of the continental lithospheric mantle. *Earth and Planetary Science Letters* **101**, 1–18.

Nelson, K. D. (1991). A unified view of craton evolution motivated by recent deep seismic reflection and refraction results. *Geophysical Journal International* **105**, 25–35.

Ochs, F. A. & Lange, R. A. (1999). The density of hydrous magmatic liquids. *Science* **283**, 1314–1317.

Parsons, T., Sleep, N. H. & Thompson, G. A. (1992). Host rock rheology controls on the emplacement of tabular intrusions: implications for underplating of extending crust. *Tectonics* **11**, 1348–1356.

Pearson, N. J., O'Reilly, S. Y. & Griffin, W. L. (1995).The crust–mantle boundary beneath cratons and craton margins: a transect across the south-west margin of the Kaapvaal craton. *Lithos* **36**, 257–287.

Petford, N. & Gallagher, K. (2001). Partial melting of mafic (amphibolitic) lower crust by periodic influx of basaltic magma. *Earth and Planetary Science Letters* **193**, 483–499.

Putirka, K. (1997). Magma transport at Hawaii: inferences based on igneous thermobarometry. *Geology* **25**, 69–72.

Ringuette, L., Martignole, J. & Windley, B. F. (1999). Magmatic crystallization, isobaric cooling, and decompression of the garnet-bearing assemblages of the Jijal sequence (Kohistan terrane, western Himalayas). *Geology* **27**, 139–142.

Ringwood, A. E. & Green, D. H. (1967). An experimental investigation of the gabbro–eclogite transformation and some geological implications. *Tectonophysics* **3**, 383–427.

Rudnick, R. L. (1992). Xenoliths—samples of the lower continental crust. In: Fountain, D. M., Arculus, R. & Kay, R. W. (eds) *Continental Lower Crust.* Amsterdam: Elsevier, pp. 269–316.

Rudnick, R. L. & Fountain, D. M. (1995). Nature and composition of the continental crust: a lower crustal perspective. *Reviews of Geophysics* **33**, 267–309.

Rudnick, R. L., McDonough, W. F., McCulloch, M. T. & Taylor, S. R. (1986). Lower crustal xenoliths from Queensland, Australia: evidence for deep crustal assimilation and fractionation of continental basalts. *Geochimica et Cosmochimica Acta* **50**, 1099–1115.

Sachs, P. M. & Hansteen, T. H. (2000). Pleistocene underplating and metasomatism of the lower continental crust: a xenolith study. *Journal of Petrology* **41**, 331–356.

Scholtz, C. H. (1990). *The Mechanics of Earthquakes and Faulting.* Cambridge: Cambridge University Press, 439 pp.

Seyler, M., Paquette, J. L., Ceuleneer, N., Kienast, J. R. & Loubet, M. (1998). Magmatic underplating, metamorphic evolution and ductile shearing in a Mesozoic lower crustal–upper mantle unit (Tinaquillo, Venezuela) of the Caribbean belt. *Journal of Geology* **106**, 35–58.

Shaw, H. R. (1980). The fracture mechanisms of magma transport from the mantle to the surface. In: Hargraves, R. B. (ed.) *Physics of Magmatic Processes.* Princeton, NJ: Princeton University Press, pp. 201–264.

Sisson, T. W. & Grove, T. L. (1993). Temperatures and $H_2O$ contents of low-MgO high-alumina basalts. *Contributions to Mineralogy and Petrology* **113**, 167–184.

Sovolev, A. V. & Chaussidon, M. (1996). $H_2O$ concentration in primary melts from supra-subduction zones and mid-ocean ridges: implications for $H_2O$ storage and recycling in the mantle. *Earth and Planetary Science Letters* **137**, 45–55.

Sovolev, A. V. & Danyushevsky, L. V. (1994). Petrology and geochemistry of the boninites from the northern termination of the Tonga trench: constraints on the generation conditions of high-Ca boninite magma. *Journal of Petrology* **35**, 1183–1211.

Spera, F. J. & Bergman, S. C. (1980). Carbon dioxide in igneous petrogenesis: I Aspect of the dissolution of $CO_2$ in silicate liquids. *Contributions to Mineralogy and Petrology* **74**, 55–66.

Stolper, E. & Walker, D. (1980). Melt density and the average composition of basalt. *Contributions to Mineralogy and Petrology* **74**, 7–12.

Suyehiro, K., Takahashi, N., Ariie, Y., Yokoi, Y., Hino, R., Shinohara, M., Kanazawa, T., Hirata, N., Tokuyama, H. & Taira, A. (1996). Continental crust, crustal underplating, and low-Q upper mantle beneath an oceanic island arc. *Science* **272**, 390–392.

Tatsumi, Y. & Eggins, S. (1995). *Subduction Zone Magmatism.* Cambridge: Blackwell, 211 pp.

Taylor, S. R. & McLennan, S. M. (1985). *The Continental Crust: its Composition and Evolution.* Oxford: Blackwell, 312 pp.

Toft, P. B., Hills, D. V. & Haggerty, S. E. (1989). Crustal evolution and the granulite to eclogite transition in xenoliths from kimberlites in the West African Craton. *Tectonophysics* **161**, 213–231.

Treloar, P. J., Brodie, K. H., Coward, M. P., Jan, M. Q., Khan, M. A., Knipe, R. J., Rex, D. C. & Williams, M. P. (1990). The evolution of the Kamila shear zone, Kohistan, Pakistan. In: Salisbury, M. H. &

Fountain, D. M. (eds) *Exposed Cross-Sections of the Continental Crust*. Dordrecht: Kluwer Academic, pp. 175–214.

Treloar, P. J., Rex, D. C., Guise, P. G., Coward, M. P., Searle, M. P., Windley, B. F., Petterson, M. G., Jan, M. Q. & Luff, I. W. (1989). K–Ar and Ar–Ar geochronology of the Himalayan collision in NW Pakistan: constraints on the timing of suturing, deformation, metamorphism and uplift. *Tectonics* **8**, 881–909.

Vervooft, J. D., Patchett, P. J., Albarède, F., Blichert-Toft, J., Rudnick, R. L. & Downes, H. (2000). Hf–Nd isotopic evolution of the lower crust. *Earth and Planetary Science Letters* **181**, 115–129.

White, R. W., Powell, R. & Clarke, G. L. (2002). The interpretation of reaction textures in Fe-rich metapelitic granulites of the Musgrave Block, central Australia: constraints from mineral equilibria calculations in the system $K_2O$–FeO–MgO–$Al_2O_3$–$SiO_2$–$H_2O$–$TiO_2$–$Fe_2O_3$. *Journal of Metamorphic Geology* **20**, 41–55.

Yamamoto, H. (1993). Contrasting metamorphic *P–T*–time paths of the Kohistan granulites and tectonics of the western Himalayas. *Journal of the Geological Society, London* **150**, 843–856.

Yamamoto, H. & Nakamura, E. (2000). Timing of magmatic and metamorphic events in the Jijal complex of the Kohistan arc deduced from Sm–Nd dating of mafic granulites. In: Khan, M. A., Treloar, P. J., Searle, M. P. & Jan, M. Q. (eds) *Tectonics of the Nanga Parbat Syntaxis and the Western Himalaya. Geological Society, London, Special Publications* **170**, 313–319.

Yamamoto, H. & Yoshino, T. (1998). Superposition of replacements in the mafic granulites of the Jijal complex of the Kohistan arc, Northern Pakistan: dehydration and rehydration within deep arc crust. *Lithos* **43**, 219–234.

Yoshino, T. & Okudaira, T. (2004). Growth and exhumation of the lower crust of the Kohistan Arc, NW Himalayas. In: Thomas, H. (ed.) *Metamorphism and Crustal Evolution*. New Delhi: Atlantic (in press).

Yoshino, T. & Satish-Kumar, M. (2001). Origin of scapolite in deep-seated metagabbros of the Kohistan Arc, NW Himalayas. *Contributions to Mineralogy and Petrology* **140**, 511–531.

Yoshino, T., Yamamoto, H., Okudaira, T. & Toriumi, M. (1998). Crustal thickening of the lower crust of the Kohistan arc (N. Pakistan) deduced from Al zoning in clinopyroxene and plagioclase. *Journal of Metamorphic Geology* **16**, 729–748.

Zandt, G. & Ammon, C. J. (1995). Continental crust composition constrained by measurements of crustal Poisson's ratio. *Nature* **374**, 152–153.